Settlement Analysis of Foundation on Weathered Rock Mass by Finite Element Method

By

Yuzo OHNISHI*

(Received December 27, 1976)

The long-term settlement of a bridge foundation was predicted by the finite element analysis. In the meantime, the collaboration of laboratory tests, in-situ tests and computer analyses was discussed and utilized in the rock mechanics analysis.

The results of the laboratory tests concluded that the creep behavior of weathered granite could be represented by a rheological model. Such a rheological model was used in the finite element analysis. The in-situ plate loading test was performed with a measurement of the strain distribution in the rock mass beneath the plate. The comparisons of the computed results and the field data indicated the effectiveness of the finite element method as far as the elastic and creep analyses are concerned. The actual bridge foundation was analyzed by the finite element method with the three-element rheological model in order to estimate the long-term settlement. The foundation structure was found to displace less than 12 cm, and it was concluded that the amount of the settlement was in the allowable range.

1. Introduction

A large foundation of a bridge has been planned on weathered rock mass in the sea water. Usually in designing the foundation, the strength and deformability of the rock mass underlying the foundation are most important. In this case, however, the rock mass is known to have enough strength and so the settlement of the foundation is considered to be most critical in constructing the bridge.

Since the foundation rock mass is deep in the water, it is impossible to conduct in-situ tests. Therefore, from the boring core data, the site of a similar geologic condition with the actual foundation rock mass was explored and selected for an in-suit plate bearing test.

Now, we will mention the overall design procedure in rock mechanics and engineer-

* Department of Transportation Engineering

ing. It is well known that the site investigation, construction of constitutive laws for rock and rock mass, in-situ tests and measurement, analysis and feasibility study of the real structures must always collaborate and these projects must be checked with each other by a well organized feed back system. For example, the results of the in-situ measurement are compared with those of the analytical methods, and any discrepancies can be corrected by modifying material properties and constitutive laws which are used in the feasibility study, so on.

According to the above mentioned procedures, the paper first describes the laboratory test and the constitutive law of weathered granite. Following the in-situ plate bearing test and measurement in a tunnel, the analytical solution by the finite element method was compared with the field measurement. Lastly, the feasibility of the foundation of the bridge was studied in the various stages of loading.

2. Laboratory Test

Triaxial compression and creep tests were performed in a drained condition for samples taken from the field test site in order to establish the constitutive law of the rock and rock mass. The rock samples were weathered and their porosities range from 3% to 10%. The uniaxial strength of the sample was more than 50 kg/cm^2. Since cracks and discontinuities existed in the sample, they may control the mechanical behavior of the rock. These cracks, however, were so small and so many that the rock samples were able to represent the behavior of the rock mass if it did not have major discontinuities.

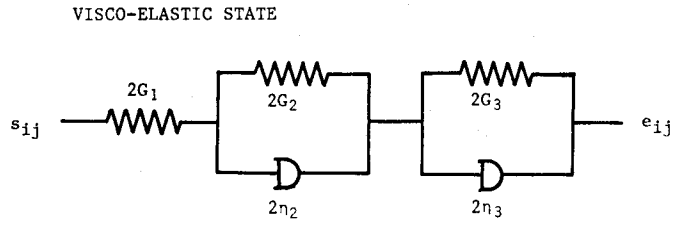

Fig. 1-a. Five-element Rheological Model.

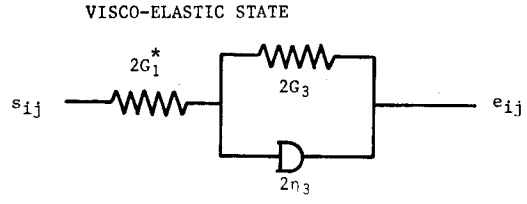

Fig. 1-b. Three-element Rheological Model (Voigt Model)

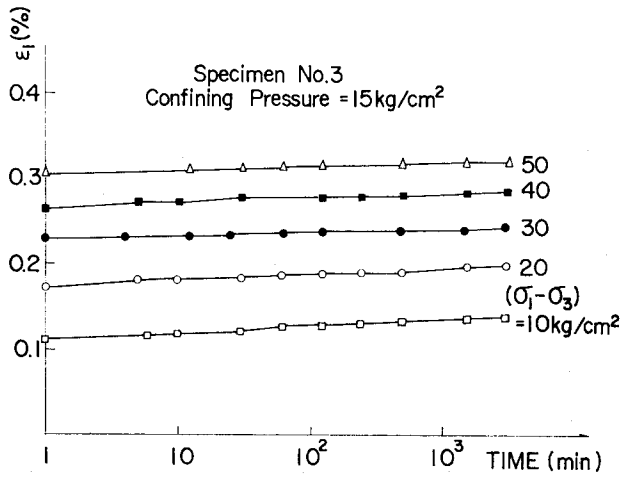

Fig. 2-a. Strain-Time Relationships under Various Deviator Stress of Weathered Granite.

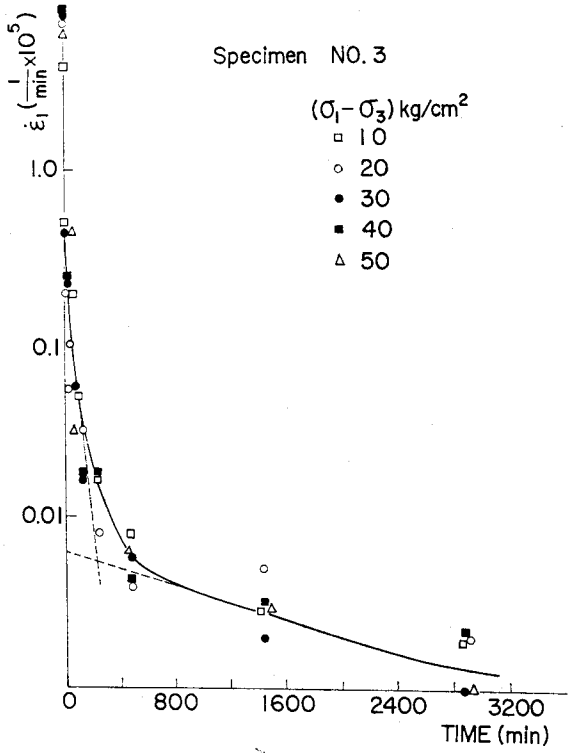

Fig. 2-b. Log Strain Rate-Time Relationships of Weathered Granite.

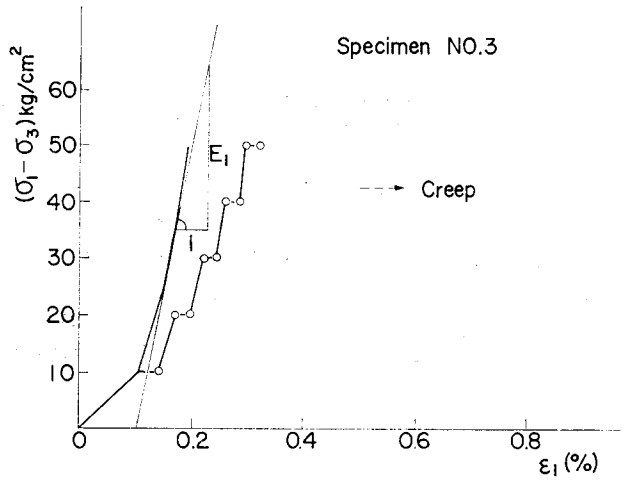

Fig. 2-c. Determination of Instantaneous Elastic Modulus.

In order to estimate the complex creep behavior of geologic materials for use in practice, a rheological model has been proposed. Rheological models have been developed in an effort to duplicate the stress-strain-time response of a material (constitutive law) in terms of various arrangements of springs, dashpots and sliders.[1)]

Recently we have proposed a five-element visco-elastic model as shown in Fig. 1-a to describe the creep deformation of weathered granite.[2)] Since the strength of the rock is found to be high enough, the state of viscoplasticity will not be considered here.

Also, in practice it may be assumed that the volumetric strain is elastic only because its time-dependency is negligible, compared with the shear deformation, in the visco-elastic state.

Fig. 2-a shows typical creep strain vs. time relationships with different stress levels for the weathered granite. Fig. 2-b is in the form of the log strain rate and time. It may be recognized that the relationship is approximated by two straight lines, each of which represents the second and third deformation element of the five-element visco-elastic rheological model. The instantaneous elastic modulus was obtained from a stress-strain curve in which the amount of creep strain was subtracted as shown in Fig. 2-c.

The constitutive equation for the rock specimen in the triaxial test is:

$$\dot{e}_{11}/s_{11}=[e^{-G_2t/\eta_2}/2\eta_2+e^{-G_3t/\eta_3}/2\eta_3]$$

where $\dot{e}_{11}$ is the rate of deviator strain, s_{11} is the deviator stress, and G_2, G_3, η_2, η_3 are the material constants which can be determined from Fig. 2-b, for example.

In computation, the five-element model is still cumbersome. If it can be assumed that the deformation due to the second deformation element ceases in a short time with

respect to the long-term deformation of the third one, the first and second deformation elements are combined and replaced by a single deformation element like a spring as shown in Fig. 1-b.

The replaced elastic shear modulus G_1^* is written as:

$$G_1^*=G_1G_2/(G_1+G_2)$$

The ratio of the total creep strain to the short-term strain is given by G_1^*/G_3. Table 1 shows the material constants obtained in the triaxial test of the weathered granite.

3. In-Situ Plate Bearing Testing

In the field of rock mechanics, in-situ tests are the most popular methods to understand the mechanical properties of rock mass. The most widely used test method for obtaining a deformation modulus for design purposes is the plate bearing test.

The plate bearing test was performed in an excavated tunnel whose geologic condition was similar to that of the actual undersea construction site.

Fig. 3 illustrates the schematic diagram of the setup for the in-situ plate bearing test. The diameter of the circular plate was 1 m and the strain gauges were buried in the drilled holes beneath the plate in order to measure the strains of the rock mass during loading.

The exploration of the test site revealed the geologic condition as shown in Fig. 4 and indicated that the rock mass was approximately divided into six layers with the assistance of the seismic logging and bore hole testing.

F.g. 5 shows a test result of the deformat.on of the plate vs. the load intensity in the plate bearing test. The creep deformation with time is shown in Fig. 6.

The strain gauges buried in the ground worked satisfactorily well. Fig. 7 shows

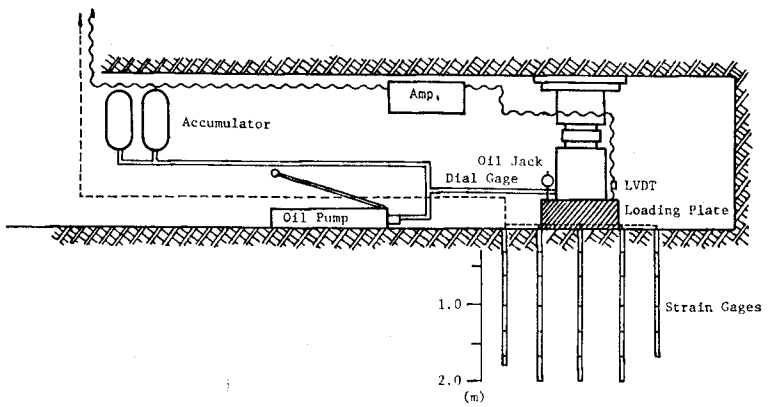

Fig. 3. Schematic Diagram of Setup for In-Situ Plate Loading Test.

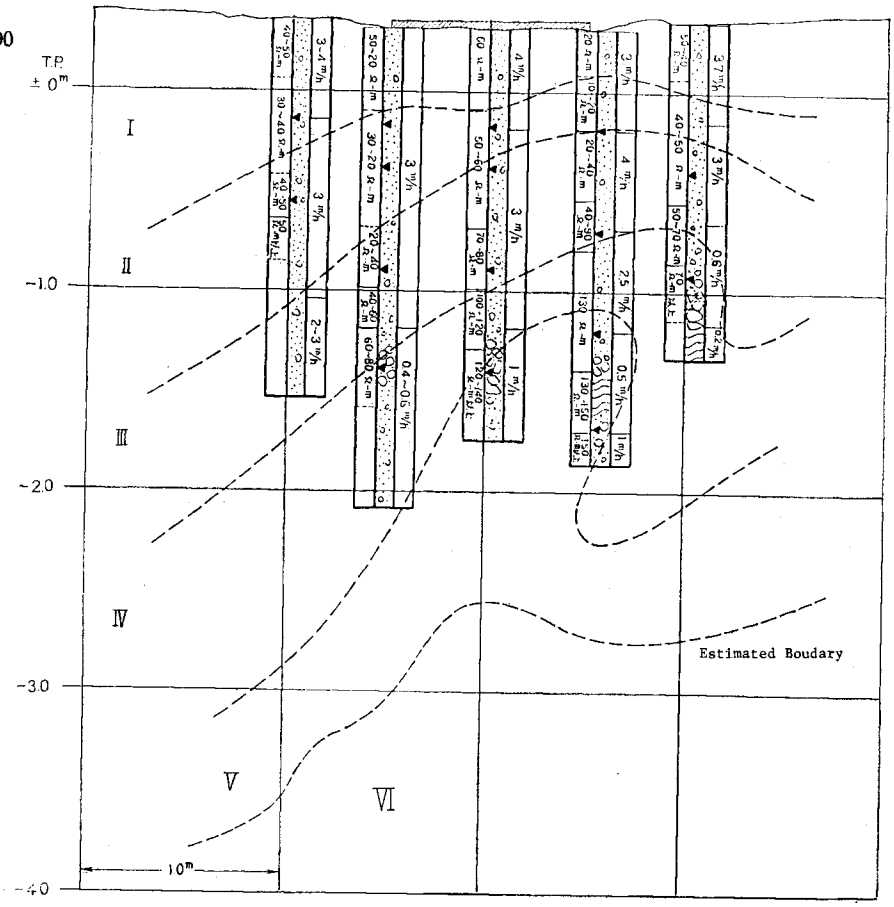

	I	II	III	IV	V	VI
Geologic Condition						
Rate of Excavation	4 m/h	3 - 4 m/h	2 - 3 m/h	0.5 ~ 2.5 m/h	0.5 ~ 1.0 m/h	
Resistivity	60 ~ 20 Ω-m	20 ~ 50 Ω-m	40 ~ 90 Ω-m	80 ~ 130 Ω-m	130~ Ω-m	
Bore Hole Jack Test E kg/cm^2	700	700 ~ 1000	1000 ~ 2000	2000 ~ 3000	3000 ~	
Average E kg/cm^2	700	1000	1500	2500	5000	10000

Fig. 4. Geologic Map of Test Site.

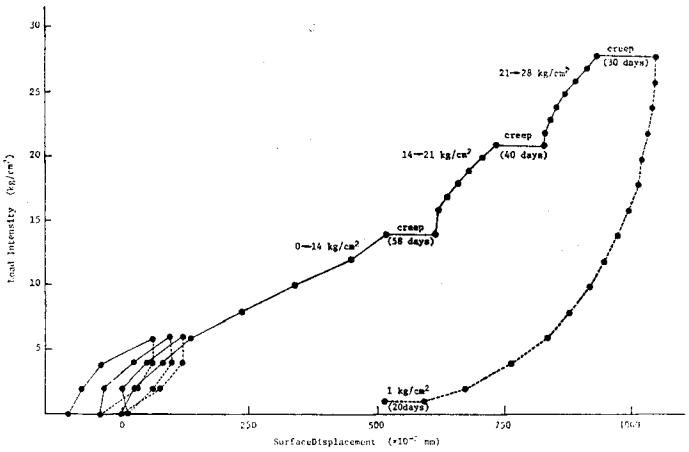

Fig. 5. Surface Displacement of Loading Plate.

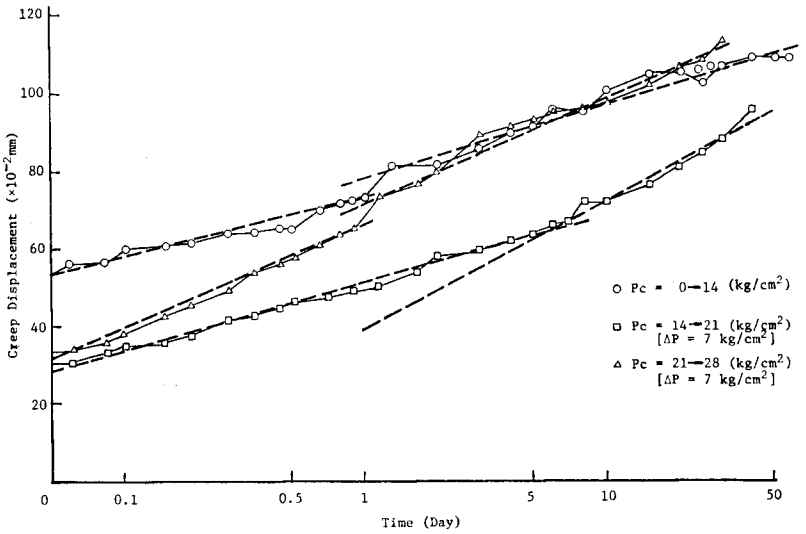

Fig. 6. Creep Displacement of Loading Plate.

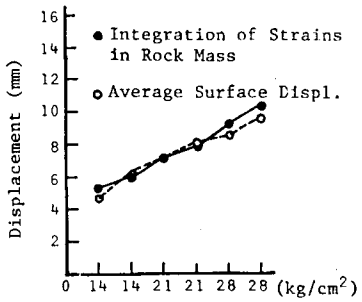

Fig. 7. Comparison between Surface Displacement and Integrated Strain in Rock Mass.

that the integration of strains from the bottom to the surface agreed very well with the average surface displacement measured by dial gauges.

4. Finite Element Analysis

The finite element analysis was performed to interpret the in-situ test results, and to understand the material properties of the weathered rock mass. A general purpose finite element code "GEOTEC"[3] was used. In the code, the "initial strain" approach

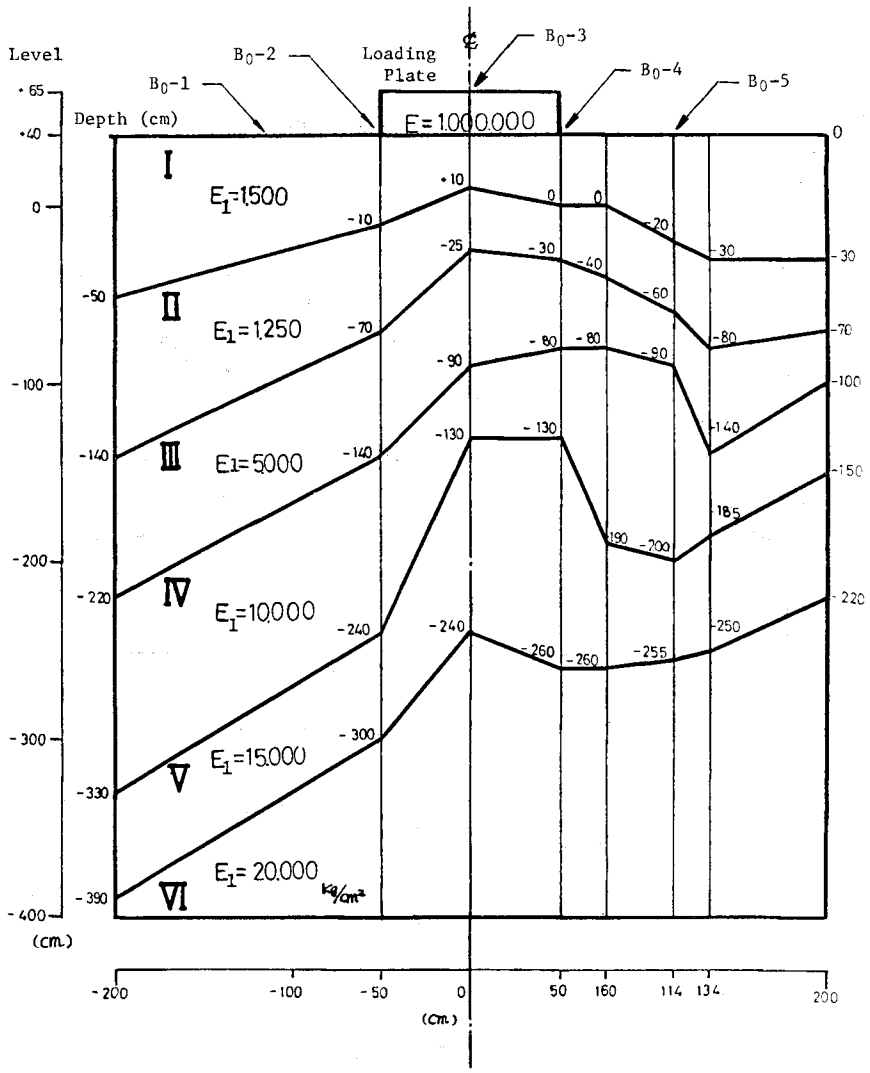

Fig. 8. Finite Element Model of In-situ Test Site.

which was suggested and utilized by Zienkiewicz, et al[4] was adopted to analyze the creep phenomenon of the rock mass.

The rock mass was idealized by a finite element model (Fig. 8) of 449 quadrilateral isoparametric elements divided into six layers. It was obtained from the geologic map of Fig. 4. Fig. 9 is an example of the comparison between the measured strain distribu-

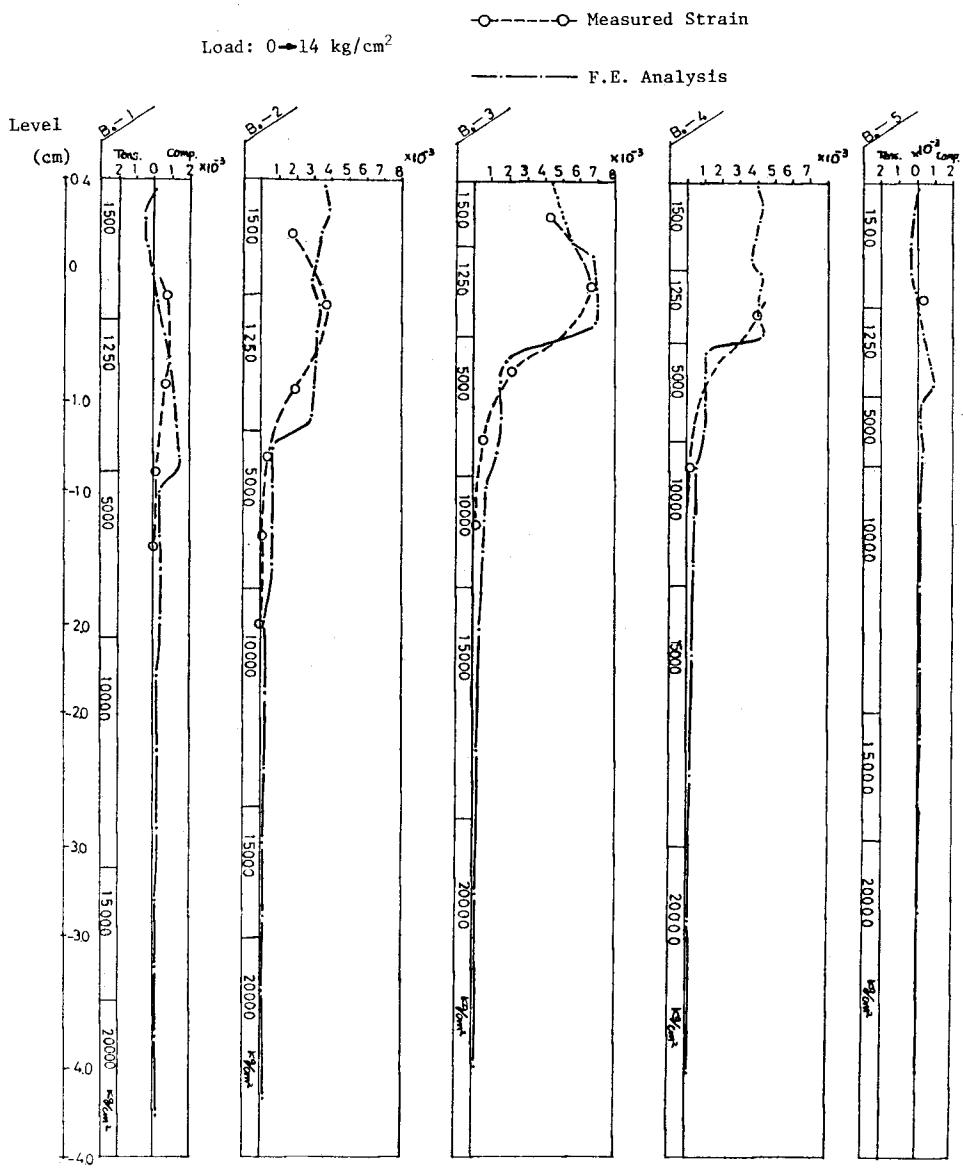

Fig. 9. Elastic Strain Distribution in Rock Mass.

tion and the analytical elastic solution. Although the loading plate was circular and axisymmetric, the plane strain analysis was done because the effects of unsymmetry and unevenness of the geologic condition were very strong. The finite element analysis was done so as to fit the solution to suit the results of the in-situ measurement as much as possible, and at the time for best fitting the material properties: for example, elastic

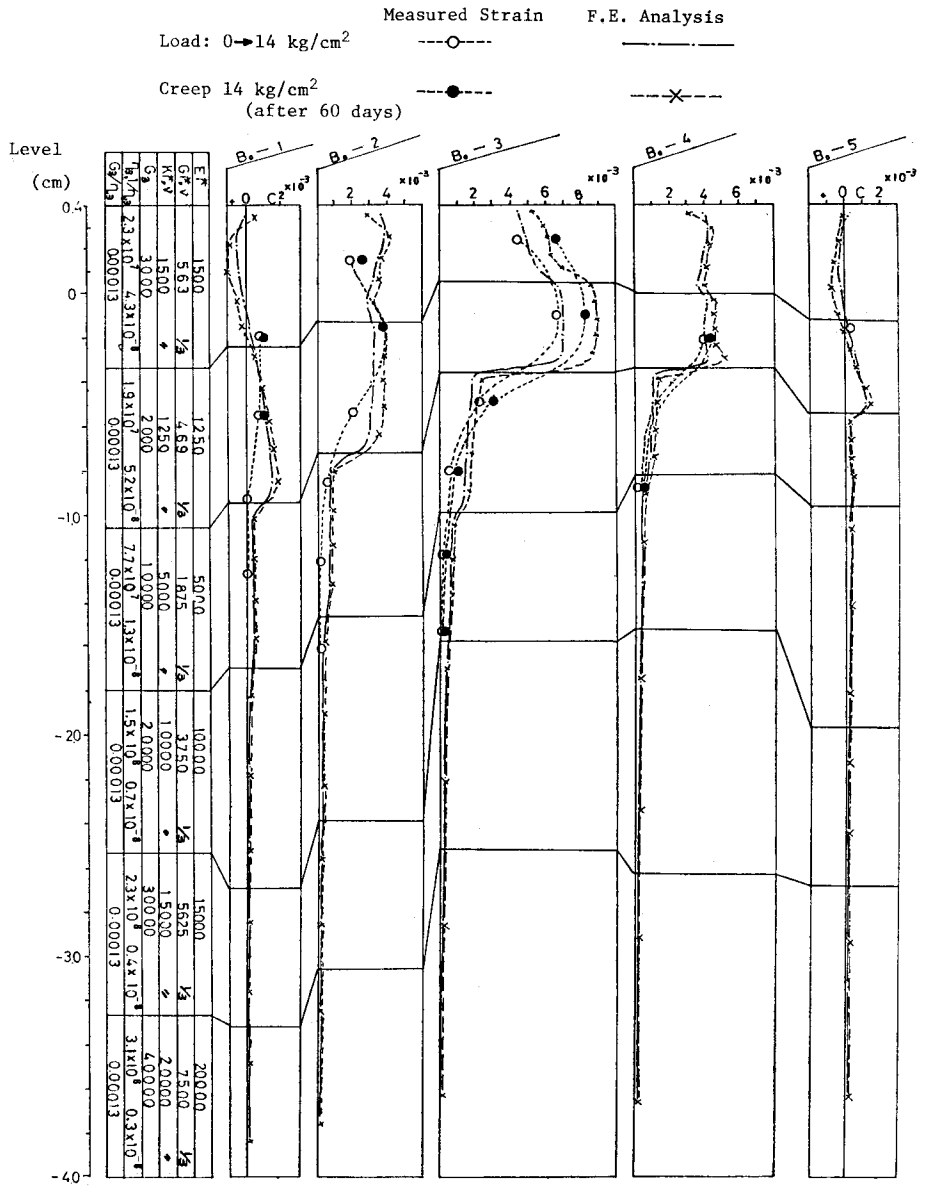

Fig. 10. Creep Strain Distribution in Rock Mass.

Table 1 Material Constants of Weathered Granite

Rock Class.	Conf. press. kg/cm	G_1 kg/cm²	G_2 kg/cm²	G_3 kg/cm²	G^* kg/cm²	η_2 kg·min./cm²	η^3 kg·min./cm²	G^*/G_3	average
C_L Class Sample	2	6.2×10^3	2.8×10^4	4.7×10^4	5.1×10^3	2.2×10^6	1.6×10^8	0.11	0.12
	10	7.5×10^3	2.9×10^4	7.5×10^4	5.4×10^3	6.3×10^5	3.7×10^7	0.07	
	15	1.9×10^4	6.7×10^4	8.5×10^4	1.5×10^4	1.1×10^7	3.7×10^8	0.17	
D Class Sample	2	2.0×10^3	2.8×10^2	1.4×10^3	2.4×10^2	1.5×10^4	7.1×10^6	0.17	0.23
	10	4.2×10^3	1.2×10^3	7.1×10^3	9.2×10^2	9.7×10^4	3.0×10^7	0.13	
	20	3.7×10^3	1.6×10^3	2.9×10^3	1.1×10^3	1.4×10^5	1.1×10^7	0.38	

moduli in Fig. 8, were considered to be close to the real values.

Results obtained from Fig. 9 indicated that the measured strains were maximum at the depth of 0.5 m (about half of the plate size) and became one tenth of the maximum values at the depth of 1.0 m (almost equal to the plate diameter). This was probably caused by the base friction of the plate and the compaction of the rock mass due to loading. Therefore, in the calculation, the elastic modulus of the surface layer is larger than that of the second. The determined elastic modulus of each layer in Fig. 8 is somewhat lower than that of the triaxial test specimen of class D in Table 1. In particular, the moduli of the upper layers are less than one tenth of the laboratory test results, probably because of the uncertainty of the geologic condition and stress relief due to the tunnel excavation, and drying the rock surface by dewatering.

A result of the creep deformation analysis by the finite element method is shown in Fig. 10. The computer results agreed very well with the measured strain distribution.

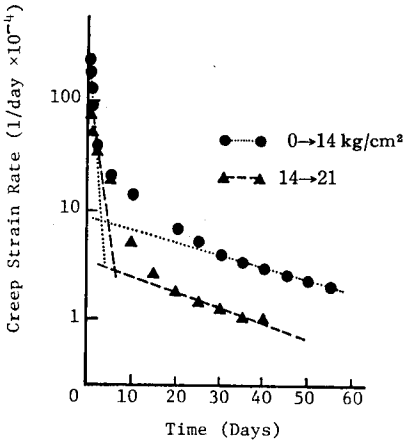

Fig. 11. Example of Log Strain Rate-Time Relationships in Rock Mass.

The material constants for the rock mass of each layer were estimated from the laboratory test and the in-situ test results. The same elastic moduli were used as in the elastic analysis. The relationship between the rate of the creep strain and the time of a measuring point in the rock mass (for example, Fig. 11), indicates that the idea which was explained in Section 2 with the rheological model can be applied in the field. Thus, the evaluated parameters for the three-element model, G_1^*, G_3, η_3 were in an order of 10^3 kg/cm^2, 10^4 kg/cm^2 and 10^8 kg/cm^{2}min, respectively. A parametric study found that in this type of the rock mass, G_3/η_3 nearly equals 1.3×10^{-4}min^{-1}.

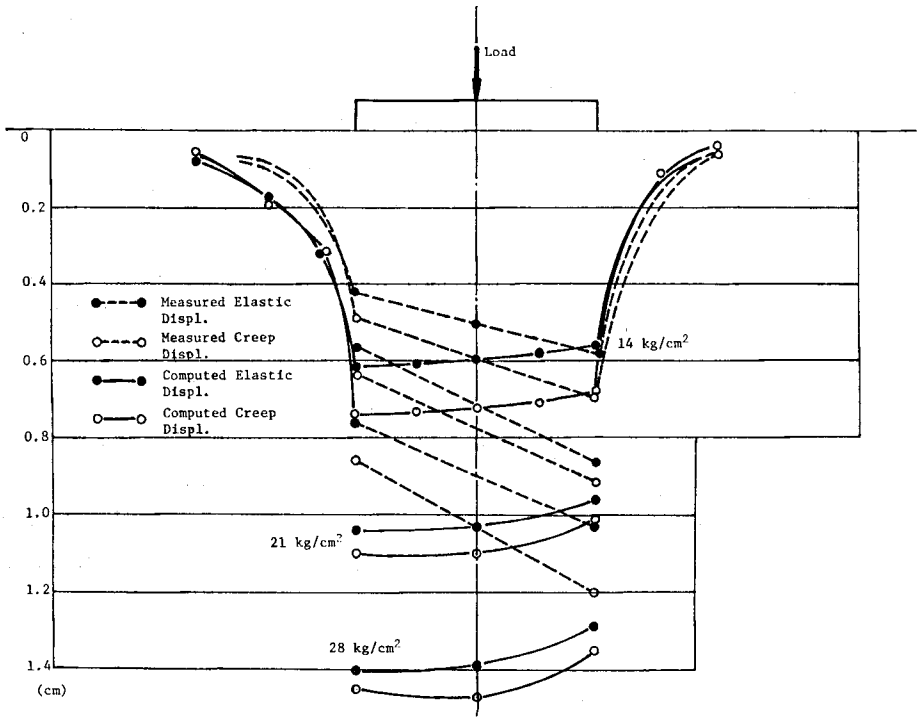

Fig. 12-a. Distribution of Surface Displacement at Three Load Steps.

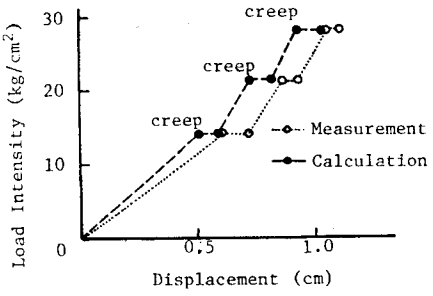

Fig. 12-b. Average Surface Displacement at Three Load Steps.

Figs. 12-a and 12-b show the settlement of the loading plate by the in-situ measurement and computation. Fig. 12-a shows the profile of the surface displacement. The measured settlement of the plate is directed in the opposite way of the results by the finite element analysis, because the actual rock mass is in three-dimension and the analysis is in plane-strain condition, and also the finite element mode does not duplicate the actual geology of the rock mass. Fig. 12-b is compatible to Fig. 5 and shows the compaction or consolidation of the rock mass with the load increase because the deformation modulus becomes larger and stiffer at each increment of loading. The amount of creep deformation by the finite element analysis is very close to the measured amount. However, in order to estimate the correct settlement, the instantaneous deformation must be calculated by a nonlinear analysis such as the theory of plasticity, since Fig. 5 shows a large permanent settlement of the plate when unloaded.

Although the plastic analysis was not performed here because of the lack of the strength parameters and the cost, the finite element analysis hitherto described is considered to be an accurate method to predict the creep behavior of the rock mass with the assistance of the in-situ test and the laboratory experiments. Hence, the construction site of a bridge fundation will be simulated by a finite element model, and the settlement of the foundation will be discussed in the next section.

5. Feasibility Study

Since the settlement of the foundation of a bridge at the time of construction completed and a long time later, say 100 years, is most critical in this case, the feasibility was studied by the finite element analysis. The block diagram of the finite element model at the construction site is shown in Fig. 13. 524 quadrilateral isoparametric elements were generated. The geologic condition and material properties were estimated with limited data from the site investigation such as boring core data, bore hold jack tests,

Table 2 Material Properties used in Finite Element Model

MAT. No.	Rock mass classification	E kg/cm²	ν	G* kg/cm²	K* kg/cm²	G_3 kg/cm²	η_3 kg·min/cm²
0	—	—	—	—	—	—	—
1	CONCRETE	250.000	0.25	100.000	166.700	—	—
2	D class	2.400	0.4	857	4.000	4.800	0.37×10^{8}
3	C_L class	10.000	0.4	3.570	16.700	20.000	0.15×10
4	C_L-C_M class	15.000	0.3	5.770	12.500	30.000	0.23×10^{9}
5	C_M class	20.000	0.3	7.690	16.700	40.000	0.31×10^{9}
6	C_H class	40.000	0.3	15.380	33.300	80.000	0.61×10^{9}
7	B class	80.000	0.3	30.770	66.700	160.000	1.23×10^{9}

$G_3/\eta_3=0.00013$

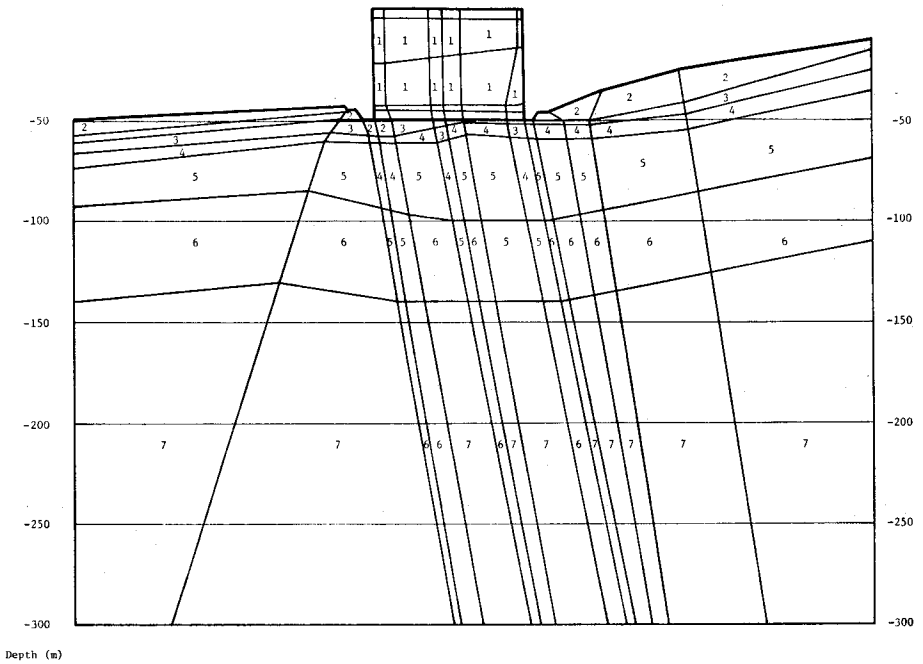

Fig. 13. Block Diagram of Finite Element Model of Actual Construction Site.

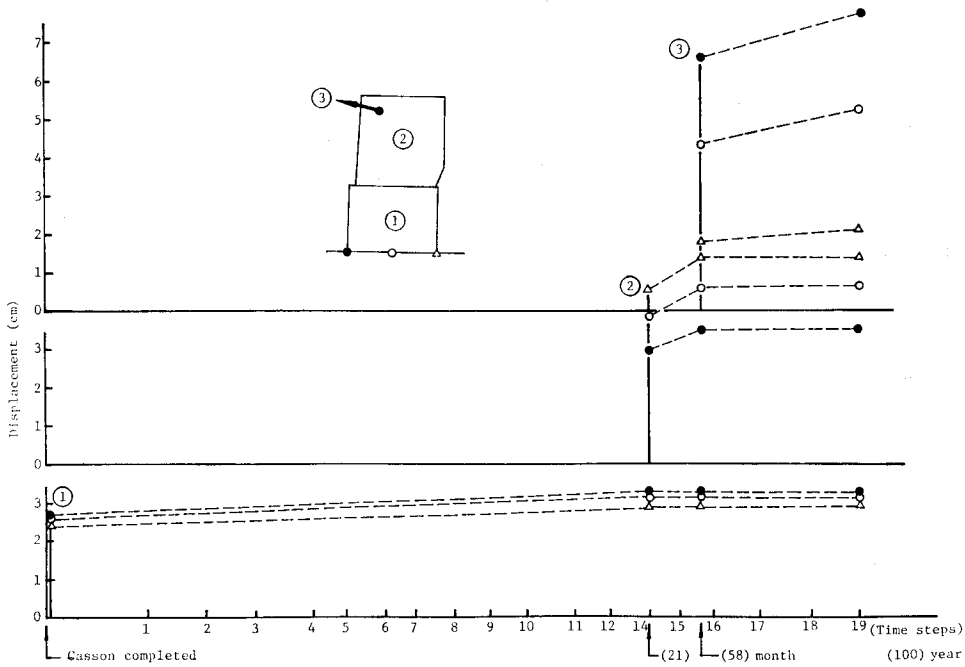

Fig. 14-a. Elastic and Creep Displacements of Structure.

the in-situ test, etc.. The material constants used are given in Table 2, and the numbers in the table correspond to the material numbers in Fig. 13. The loading conditions of the analysis were as follow:

First step: at the time the caisson was completed

Second step: at the time the anchorage was constructed

Third step: at the time the cables was tensioned and the bridge construction was completed

At each load step, the equivalent force was calculated and applied to appropriate nodal points. Fig. 14-a shows the elastic and creep deformation at each load step. The calculated ratio of creep deformation to elastic deformation for the foundation is about 0.2, and is nearly equal to the in-situ test result. The displacement of the foundation structure is illustrated in Fig. 14-b. The maximum vertical displacement is less than 12 cm and may be in the allowable range. However, since the effects of consolidation and the plastic deformation were not considered here, in the design procedure such factors must be examined.

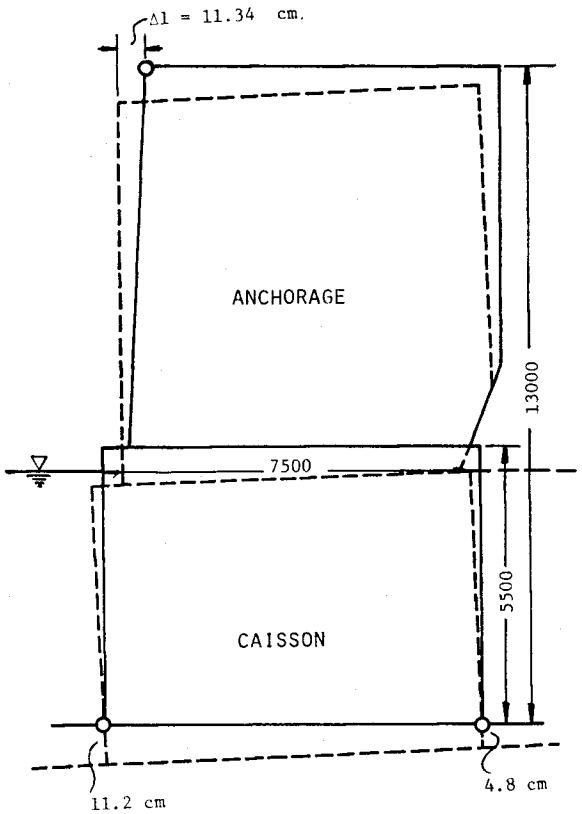

Fig. 14-b. Final Displacement of Structure.

6. Conclusions

The main object of this study was the prediction of the long-term settlement of a bridge foundation on a weathered rock mass. However, in the process, we were carefully concerned with the collaboration of laboratory tests, in-situ tests and computer analyses. We believe only such a co-operated feed back system can stimulate the progress of rock mechanics and engineering.

The laboratory tests deduced the conclusion that the creep behavior of weathered granite could be represented by a rheological model. The three-element rheological model was found to be simple and accurate enough, and so was used in the finite element method to analyze the in-situ plate loading test. The in-situ test was carried out in a tunnel, with a measurement of the strain distribution in the rock mass. The comparisons of the computed results and the field data indicated the effectiveness of the finite element analysis as far as the elastic and creep behaviors are concerned.

The feasibility study of the actual foundation was performed by the finite element method, and within the limited geological data it was known that the settlement of the structure would be less than 12 cm and may be in the allowable range. However, it should be noted that the actual rock mass, as in the in-situ test, showed more complicated behaviors, such as consolidation, compaction and plastic deformation. In order to analyze those nonlinear behaviors, much more elaborate tests and analyses must be achieved.

Acknowledgements

The work described in the paper was sponsored by the Honshu-Shikoku Bridge Authority. The author would like to thank Prof. K. Akai and Prof. T. Adachi in Kyoto Univ., without whose encouragement, advice and assistance much of this work would never have been completed. Thanks are also to Prof. K. Yamamoto, Messrs. T. Takeuchi, H. Kishimoto for their helpful advice and assistance.

References

1) Mitchel, J. K.: "Fundamentals of Soil Behavior," John Wiley & Sons (1976).
2) Akai, K., Adachi, T., Yamamoto, K. and Ohnishi, Y.: Memoirs of Faculty of Engineering, Kyoto Univ., Vol. 39-1 (1977).
3) Ohnishi, Y. and Kishimoto, H.: "GEOTEC: A General Program For Geotechnical Engineering" Report, Division of Geotechnical Eng., Dept. of Civil Engineering, Kyoto Univ. In Press.
4) Zienkiewicz, O. C., Watson, M., and King, I.: Int. J. of Mech. Sci., Vol. 10 (1968).